

## Ionic liquid-assisted synthesis, characterization and photocatalytic properties of SnO microflowers with nanosheet subunits

Masoomeh Siminghad, Ashraf S. Shahvelayati\*, Shabnam Sheshmani\*, Roya Ahmadi

Department of Chemistry, Yadegar-e-Imam Khomeini (RAH) Shahre-rey Branch, Islamic Azad University, Tehran, Iran

Received: 2019-05-24

Accepted: 2019-07-15

Published: 2019-09-20

### ABSTRACT

In this study, simple ionic liquid-assisted preparation of SnO microflowers with nanosheet subunits under reflux condition without calcination were described. Samples were synthesized using 1-pentyl-3-methylimidazolium bromide, [pmim]Br, as an ionic liquid in different molar ratio, sodium hydroxide and Tin(II) chloride. The results show that SnO with high purity and uniform size distribution was obtained using 1:4:4 molar ratios of SnCl<sub>2</sub>/NaOH/IL by simple reflux method and the ionic liquid only acts as a suitable template. The characterization of the products was carried out by FT-IR, X-ray powder diffraction (XRD), scanning electron microscopy (SEM), energy dispersive X-ray spectroscopy (EDXS) and DRS techniques. Photodegradation of Remazol Black B (RBB) from the aqueous solution was investigated by SnO nanosheets (93.48% dye removal). The rate of degradation of RBB in the presence of SnO is distinctive by the pseudo-first-order kinetic model ( $R^2 > 0.79$ ).

**Keywords:** 1-Pentyl-3-methylimidazolium bromide; Ionic liquid; Microflower; Nanosheet; Photodegradation; Remazol Black B; SnO

© 2019 Published by Journal of Nanoanalysis.

### How to cite this article

Siminghad M, Shahvelayati AS, Sheshmani S, Ahmadi R. Ionic liquid-assisted synthesis, characterization and photocatalytic properties of SnO microflowers with nanosheet subunits. J. Nanoanalysis., 2019; 6(4): 228-236. DOI: 10.22034/jna.\*\*\*

## INTRODUCTION

In the recent decades, much effort has been made toward the synthesis and characterization of nanosized transition metal oxide particles. One of them is Tin(II) oxide (stannous oxide) that contains two forms, a stable black and a meta stable red form. Tin oxide is widely studied, due to its potential applications as gas-sensing material, antistatic film, thin film resisters, anti-reflecting coating in solar cell and p-type semiconductor with wide direct optical band gap of 2.5-3.4 eV [1-4]. Different methods for the preparation of tin oxide have been reported such as *e.g.*, precipitation, sol-gel, sonochemical, microwave, solvothermal, spray pyrolysis, pulsed laser deposition, sputtering and deposition [5-12]. For example, Dai et al. used thermal evaporation to synthesize diskettes-

like SnO crystals [13]. Orlandi et al. employed vapor-liquid-solid methods to synthesize belts and dendrites like SnO crystals [14]. Uchiyama et al. used acidic aqueous solution to manipulate the SnO morphology [15]. Nano-square sheets [16] and sheets-like [17] SnO were synthesized by template-free hydrothermal growth method and chemical vapor deposition (CVD), respectively. However, some techniques required complicated experimental method with high temperature equipment. Also, there are some environmental aspects of the synthesis procedure. It was significant to develop a simple and environmentally method for preparation of nanostructured SnO. One of the new methods that have been recently considered is the use of ionic liquids (ILs) as potential templates. Room temperature ionic liquids (RTILs), especially

\* Corresponding Author Email: [avelayati@yahoo.com](mailto:avelayati@yahoo.com)



those based on 1,3-dialkylimidazolium salts, have shown great promise as attractive alternatives to the conventional solvents. Ionic liquids (IL) are receiving increasing interest in nanomaterials synthesis due to their properties such as thermal and chemical stability, negligible vapor pressure, immiscibility with both organic and inorganic compounds, non-flammability and recyclability [18, 19]. It is well recognized that the physical properties of a material strongly depends on its size and morphology. ILs have been widely used as templates for the synthesis of nanomaterials. By modifying the structure of the cations or anions of ionic liquids, it has been shown that their properties can be altered in order to influence on morphology, size and optical properties of nanomaterials [20].

Until now, various kinds of metal oxide semiconductor materials such as SnO have been used as a photocatalyst in degradation of dye pollutants [21-25]. However, many researchers have reported that the properties of semiconductors depend on to their crystalline structure, size, and morphology, but achieving high photocatalyst activity is still a challenge [26, 27].

As a part of our continuing efforts toward the development of novel, efficient, and green procedures in the rapid ionic liquid assisted synthesis of nanometal oxides [28-30], in this article, nanosheet morphologies of SnO structures have been successfully synthesized by a simple reflux method in water in the presence of 1-pentyl-3-methylimidazolium bromide as an ionic liquid. Different molar ratios of 1-pentyl-3-methylimidazolium bromide and sodium hydroxide were dissolved in water and used as a reaction medium for preparation of SnO nanostructure without calcination.

In recent years, large numbers of photocatalysts, such as ZnO [31], TiO<sub>2</sub> [32, 33], SnO<sub>2</sub> [34], MnO<sub>2</sub>, Mn<sub>3</sub>O<sub>4</sub> [35] and CuO [36] were investigated in RBB photodegradation. The degradation efficiency was observed above 90% in most cases under irradiation of UV light. In this research, photocatalytic properties of the synthesized SnO under visible light irradiation were investigated in degradation of Remazol Black B (RBB). Some factors affecting such as pH, adsorbent dosage, dye concentration and contact time, were studied to optimize the photodegradation conditions. The kinetic of the photocatalytic process of these nanocomposites was also evaluated.

## EXPERIMENTAL

### Materials

1-Bromopentane (C<sub>5</sub>H<sub>11</sub>Br, 99%), 1-methylimidazole (C<sub>4</sub>H<sub>6</sub>N<sub>2</sub>, 99%), tetrahydrofuran (C<sub>4</sub>H<sub>8</sub>O, 99.9%), diethyl ether) C<sub>4</sub>H<sub>10</sub>O (were purchased from Sigma-Aldrich (Germany). Tin(II) chloride (SnCl<sub>2</sub>, 99.9%), Sodium hydroxide (NaOH, 97%), absolute ethanol (C<sub>2</sub>H<sub>5</sub>OH), were brought from Merck Ltd (Germany). Remazol Black B (RBB) was obtained from Alvand Sabet Company (Iran). All chemicals were commercially available analytical grade and were used without further purification.

### Preparation of 1-pentyl-3-methylimidazolium bromide ionic liquid

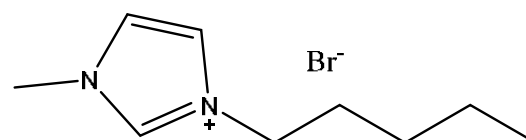
The IL used in this study was synthesized according to Menshutkin reaction [37]. For synthesis of 1-pentyl-3-methylimidazolium bromide, a mixture of N-methylimidazole (10 mmol, 0.79 mL) and 1-bromopentane (10 mmol, 1.24 mL) was refluxed for 6 hours in THF under N<sub>2</sub>. The viscose liquid was washed repeatedly with THF (3 × 10 mL). The solvent from the mixture was evaporated under reduced pressure to leave the colorless viscose oil as an ionic liquid. <sup>1</sup>H NMR and IR spectroscopic data are used to confirm the structure of ionic liquid (Scheme 1).

1-Pentyl-3-methylimidazolium bromide [pmim] Br:

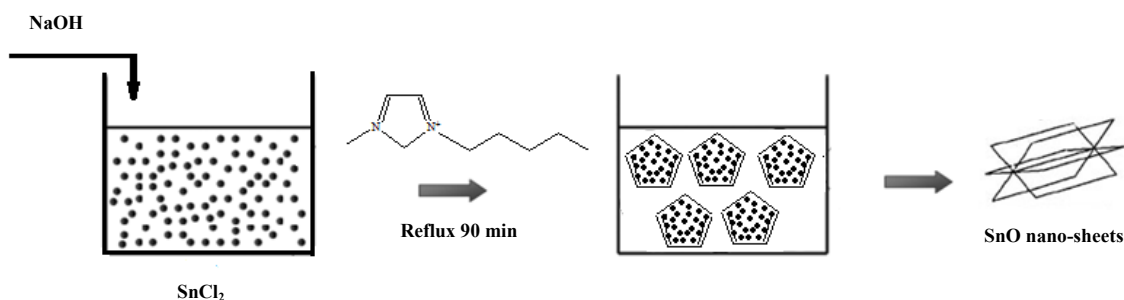
Viscous oil, Yield: (98%), IR (cm<sup>-1</sup>) (KBr): 3051, 2929, 2860, 1632, 1490, <sup>1</sup>HNMR (500 MHz, CDCl<sub>3</sub>) δ = 0.88 (3 H, t, <sup>3</sup>J = 6.5, CH<sub>3</sub>), 1.27-1.32 (6 H, m, 3CH<sub>2</sub>), 3.66 (3 H, s, NCH<sub>3</sub>), 3.95 (2 H, t, <sup>3</sup>J = 6.5, NCH<sub>2</sub>), 7.24 (2H, s, 2 CH); 9.54 (1H, s, CH) ppm.

### Preparation of SnO

A simple approach used in the preparation of SnO nanosheet is reflux protocol. In this method, SnCl<sub>2</sub> were converted to form nanosheet by the using of ionic liquid (Scheme 2). The reaction between SnCl<sub>2</sub> with sodium hydroxide in the presence and absence of 1-pentyl-3-methylimidazolium bromide at reflux temperature without calcination



Scheme 1. Structure of 1-pentyl-3-methylimidazolium bromide [pmim]Br



Scheme 2. Illustration for the processes of SnO nanosheets synthesized by IL-assisted growth

leads to a preparation of SnO with different size and morphology. The reaction mixture was transferred into a round bottom flask and refluxed for 90 min. After the reaction was complete, the resulting black solid product was washed with distilled water and ethanol. The different molar ratio of SnCl<sub>2</sub>/NaOH and SnCl<sub>2</sub>/NaOH/IL as 1:3, 1:4 and 1:3:4 and 1:4:4 were studied in SnO preparation.

#### Characterizations

Fourier transform-infrared measurements (FT-IR) spectra were recorded (between 500 and 4000 cm<sup>-1</sup>) on KBr pellets with a Tensor 27 Bruker spectrophotometer. <sup>1</sup>H and <sup>13</sup>C NMR spectra were recorded with a Bruker DRX-300 Advance instrument using CDCl<sub>3</sub> as the deuterated solvent containing tetramethylsilane as internal standard, at 500 MHz, δ in ppm, J in Hz. The crystallographic structures were observed by X-ray diffraction (XRD, PHILIPS/ PW1800) at room temperature with Cu Kα radiation. The morphologies were analyzed by a scanning electron microscope (SEM, TESCAN HV:20.00kV\MIRA) that was equipped with an energy-dispersive X-ray analysis (EDXS) system. The optical properties of the samples were analyzed by UV/Vis diffuse reflectance spectroscopy (UV-vis DRS) using an Avaspec-2048-TEC spectrophotometer equipped with an integrating sphere attachment. Barium sulfate was used as a reference. The reflectance spectra were converted to equivalent absorption Kubelka-Munk units of the instrument software. The band gap was determined from the plots of transformed Kubelka-Munk as a function of the energy. UV-vis absorption spectroscopy measurements were performed by means of a Varian-Cary Bio 100 UV/V spectrophotometer.

#### Photocatalytic properties study

The effects of various parameters such as pH,

adsorbent dosage, dye concentration and contact time on the photodegradation of RBB were investigated. The solution of Remazol Black B (RBB) dye was prepared by dissolving of analytical grade dye (1 g in 1000 mL of distilled water). All experiments were carried out at room temperature (25 ± 1 °C) using a constant agitation speed of 1000 rpm. Experimental solutions of the desired concentrations were prepared by successive dilutions. All the experiments were carried out in a batch system in order to evaluate the effects of different variables. Tin (II) oxide (5 mg), was dispersed in an aqueous solution of RBB dye (20 ppm, 15 mL) in a conical flask. The reactor was stirred constantly and then irradiated by Mercury lamp at room temperature. The absorbance measurement of the reaction solution was taken after separating the adsorbent from the reaction system by centrifugation. The initial and final RBB concentrations remaining in the solutions were analyzed by a UV spectrophotometer. The photocatalytic activity was evaluated on the basis of the decrease of the absorbance band of the RBB at 597 nm. The adsorption capacity,  $q_{\max}$ , at the time (t) was calculated from the mass balance, given by Eq. (1):

$$q_t = \frac{(C_0 - C_t)V}{W} \quad (1)$$

Where  $q_t$  is the amount of dye taken up by the photocatalyst (mg/g),  $C_0$  is the initial dye concentration (mg/L),  $C_t$  is the concentration of dye (mg/L) at time t, V is the volume of dye solution (L) in contact with the adsorbent, and W is the mass (g) of the photocatalyst.

## RESULTS AND DISCUSSION

#### IR Spectrum

Fig. 1 shows the FT-IR spectrum of prepared SnO. One peak at 528 cm<sup>-1</sup> can be observed, which

is ascribed to the stretching vibrations of the Sn–O. The absorption band at  $3421\text{ cm}^{-1}$  is attributed to O–H stretching vibration of adsorbed water. The presence of ionic liquid molecules in this compound was not confirmed by IR spectroscopy because 1-pentyl-3-methylimidazolium bromide only acted as a template. Therefore, the FT-IR results, certify ensures us of the formation of SnO.

#### XRD patterns

Fig. 2 shows XRD patterns for S1-S4 samples. The S1 and S2 samples synthesized in the absence of ionic liquid with different molar ratios of  $\text{SnCl}_2 \cdot 2\text{H}_2\text{O}/\text{NaOH}$  in 1:3 and 1:4, respectively. When the molar ratio of  $\text{SnCl}_2/\text{NaOH}$  was 1:3, the XRD results confirmed the formation of SnO minor phase as well as  $\text{Sn}_{21}\text{Cl}_{16}(\text{OH})_{14}\text{O}_6$ , which were not well crystallized (Fig. 2a). When the

amount of NaOH in reaction medium increases ( $\text{SnCl}_2/\text{NaOH}$  molar ratio is 1:4) the crystalline nature of SnO with orientation in (001), (101), (110), (002), (200), (112) and (103) planes at  $18.39$ ,  $29.86$ ,  $33.30$ ,  $37.27$ ,  $47.91$ ,  $50.83$  and  $57.40^\circ$  values were observed. Therefore, SnO crystal growth is highly affected by the amount of NaOH in synthesis medium (Fig. 2b). On the other hand, S3 and S4 samples were prepared in the presence of ionic liquid. The impurity phase of Cassiterite  $\text{SnO}_2$  and minor phase of Romarchite SnO were obvious in the S3 sample, where the reaction was carried out in the 1:3:4 molar ratio of  $\text{SnCl}_2/\text{NaOH}/\text{IL}$ . The XRD pattern of S4 sample showed the crystals of SnO with a tetragonal Romarchite structure that were prepared in the 1:4:4 molar ratio of  $\text{SnCl}_2/\text{NaOH}/\text{IL}$ . No characteristic peaks of impurities were detected in the XRD pattern. The XRD

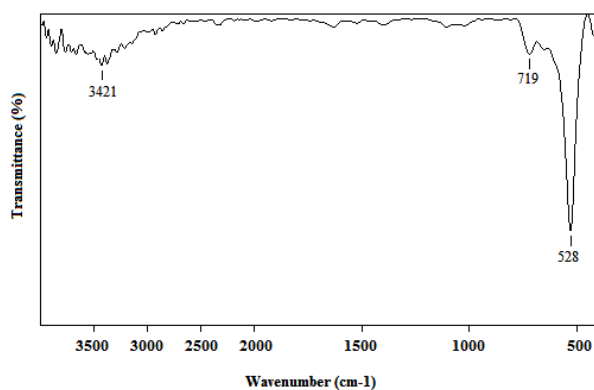


Fig. 1. FT-IR spectrum of SnO.

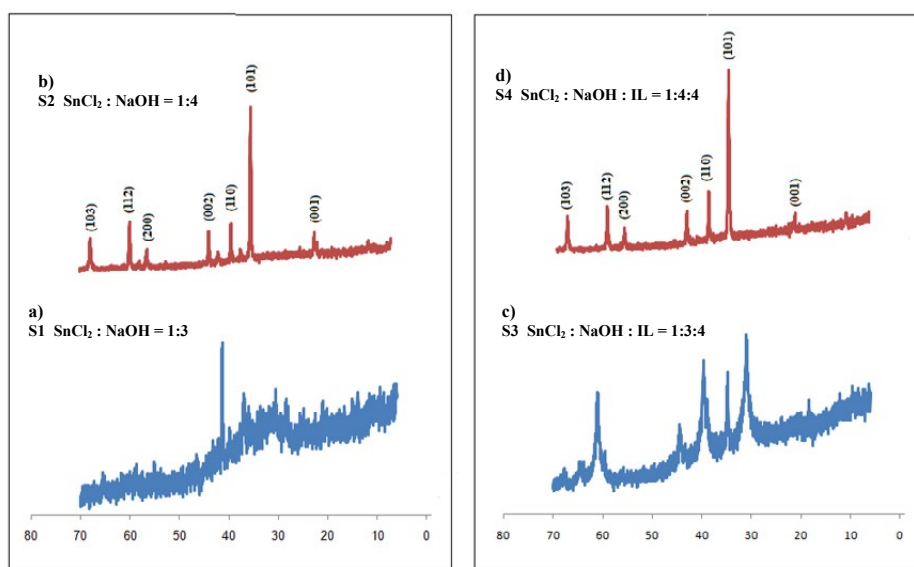


Fig. 2. XRD patterns of S1-S4 samples.

pattern of SnO can be indexed to orthorhombic lattice in the space group *Pcam* with the parameters of  $a = 5.4903\text{\AA}$ ,  $b = 5.89200\text{\AA}$ ,  $c = 4.75200\text{\AA}$ ,  $Z = 4$ . (JCPDS card file No. 36-1451).

#### SEM and EDXS Analysis

The morphology of the prepared SnO structures from the reaction between  $\text{SnCl}_2$  and sodium hydroxide via the reflux method in the absence and presence of ionic liquid are indicated in Fig. 3. In addition, energy-dispersive X-ray analysis results are given in Fig. 4.

Fig. 3a shows the obtained structure in the 1:3 molar ratios of  $\text{SnCl}_2/\text{NaOH}$  without ionic liquid. It is clear; the product mainly consists of amorphous morphology with small cubic micro-crystals. By

increasing sodium hydroxide in reaction media, small amounts of irregular SnO microsheets with an average diameter of  $0.68\text{-}1\mu\text{m}$  were obtained (Fig. 3b). When  $\text{SnCl}_2/\text{NaOH}/\text{IL}$  molar ratio is 1:4:4, nanosheet-like SnO was obtained (Fig. 3c). SEM micrograph indicated that this compound consists of nanosheets with a thickness of  $60\text{ nm}$ . Therefore, ionic liquid as a template was influenced by the thickness of the sheets, decreasing from  $0.68\text{-}1\mu\text{m}$  to  $60\text{ nm}$ . Therefore, 1-methyl-3-pentylimidazolium bromide acted as a template to yield the decrease in size and regular sheet morphology of SnO crystallites. It is well known that, a convenient way to prepare small sized particles is to add a template, such as ionic liquids. In general, there are two steps in the formation of nanostructures: first, a large

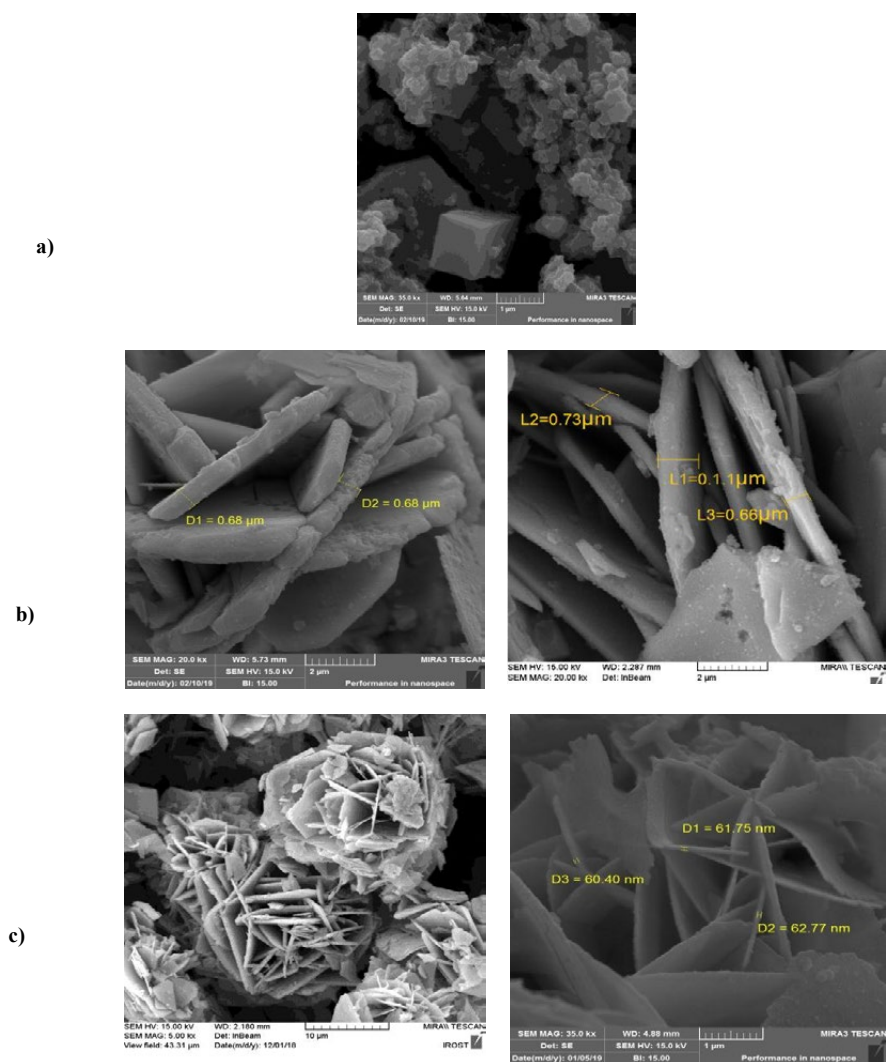
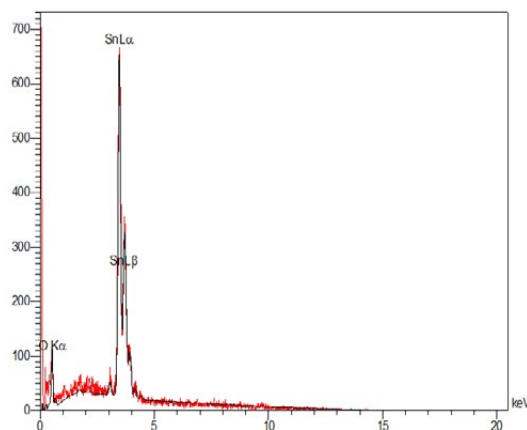


Fig. 3. SEM Micrograph a) 1:3 molar ratio of  $\text{SnCl}_2/\text{NaOH}$  without IL, b) 1:4:3 molar ratio of  $\text{SnCl}_2/\text{NaOH}/\text{IL}$  and c) 1:4:4 molar ratio of  $\text{SnCl}_2/\text{NaOH}/\text{IL}$ .



Elt	Line	Int	Error	K	Kr	W%	A%	ZAF	Formula	Ox%	Pk/Bg	Class	LConf
O	Ka	26.7	9.3407	0.0612	0.0480	19.96	64.92	0.2406		0.00	16.39	A	
Sn	La	291.6	1.1643	0.9388	0.7370	80.04	35.08	0.9208		0.00	24.08	A	
				1.0000	0.7851	100.00	100.00			0.00			

Fig. 4. Energy-dispersive X-ray analysis of SnO nanosheet.

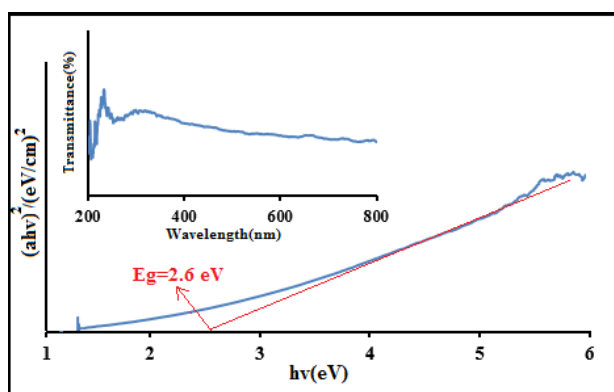


Fig. 5. Plot of transformed Kubelka - Munk as a function of the energy of light and correlation between band gap energy for SnO nanosheet.

crystal nucleus is formed and second, the growth of the formed nucleus. When a template is used in the synthesis procedure, further growth of the crystals was hindered, probably because of the adsorption of the surface-active agent on the surface of the crystal nucleus. The EDX analysis indicated 80.04 W% Sn and 19.96 W% O.

#### DRS Studies

The band gap energy can be estimated on according to following Eq. (2):

$$\alpha h\nu = B(h\nu - E_{bg})^2 \quad (2)$$

Where  $\alpha = (1-R)^2/2R$ , R is the reflectance of

the “infinitely thick” layer of the solid [38], B is the absorption coefficient, and  $h\nu$  is the photon energy in eV. Fig. 5 plots the relationship of  $(\alpha h\nu)^{1/2}$  versus photon energy ( $h\nu = 1239/\lambda$ ) [39, 40], which shows that the band gap of SnO is 2.6 eV.

#### Effect of variable parameters on the photodegradation activity

The effect of various parameters on the photodegradation of RBB in aqueous solution is shown in Fig. 6. The solution pH is the key factor in the photocatalytic reaction. To study the effect of pH on photodegradation, experiments were carried out in a pH range of 3 to 9. Fig. 6(a) showed the relationship between the pH value and the dye

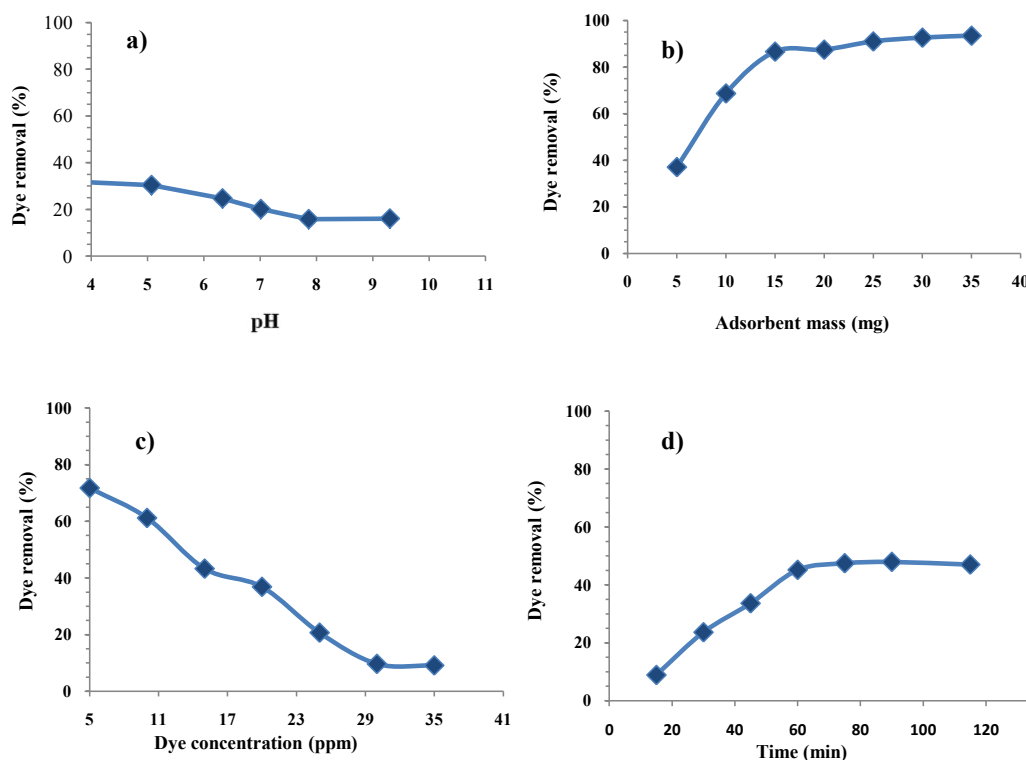


Fig. 6. Effect of a) pH value, b) adsorbent mass, c) dye concentration and d) contact time on RBB removal.

removal of RBB. Maximum dye removal value was reached at pH 5.0 (30.4%). Therefore, at acidic and/or neutral conditions, the interaction between a positively charged photocatalyst surface and negatively charged dye favors adsorption. In an alkaline condition, the adsorption capacity of RBB decreased because the charge of the photocatalyst surface was more negative.

A series of experiments were carried out to find the optimum amount of the photocatalyst by varying the photocatalyst weight between 5 and 35 mg. Fig. 6(b) shows dye removal vs. the adsorbent dosage. As can be seen, the dye removal increases as the weight of the photocatalyst increases. Maximum value (93.5%) was obtained at 35 mg of the SnO photocatalyst. With a greater amount of photocatalyst, there is an increase in the active sites.

The effect of the dye concentration is an important parameter in photocatalytic activity. Fig. 6(c) shows the photocatalytic degradation of RBB at different dye concentrations in the range 5-35 ppm. It is clear that the photodegradation of RBB decreases with increasing concentration of the dye. By increasing the concentration of RBB, more dye molecules are adsorbed at the photocatalyst surface, resulting in the occupation of the catalyst active

sites and consequently decreasing the photocatalyst surface. The effect of contact time (15-120 min) was studied in the photodegradation of RBB. The results reveal that the photodegradation increases with the extension of contact time to 60 min and then remained constant (Fig. 6(d)).

#### Kinetic studies

The rate of degradation of RBB in the presence of SnO is distinctive by the pseudo-first-order kinetic model as proposed by Eq. (3). Where  $C_0$  is the initial concentration,  $C_t$  is the concentration over time ( $t$ ), and  $K$  is rate constant of pseudo-first-order ( $\text{min}^{-1}$ ). The value of  $K$  was determined from the slopes of the plot of  $\ln(C_0 - C_t)$  vs.  $t$  (Fig. 7).

$$\ln(C_{t(CO)} = Kt) \quad (3)$$

#### Regeneration and reuse of SnO

The regeneration and reuse of photocatalysts is quite crucial in practical applications because ecological and economic demands. It is observed that SnO can be subjected to multiple rounds of reuse (Fig. 8). The photocatalytic capacity decreases for each new cycle. Meanwhile, after four cycles, the photocatalytic capacity reached at 48.2%. These

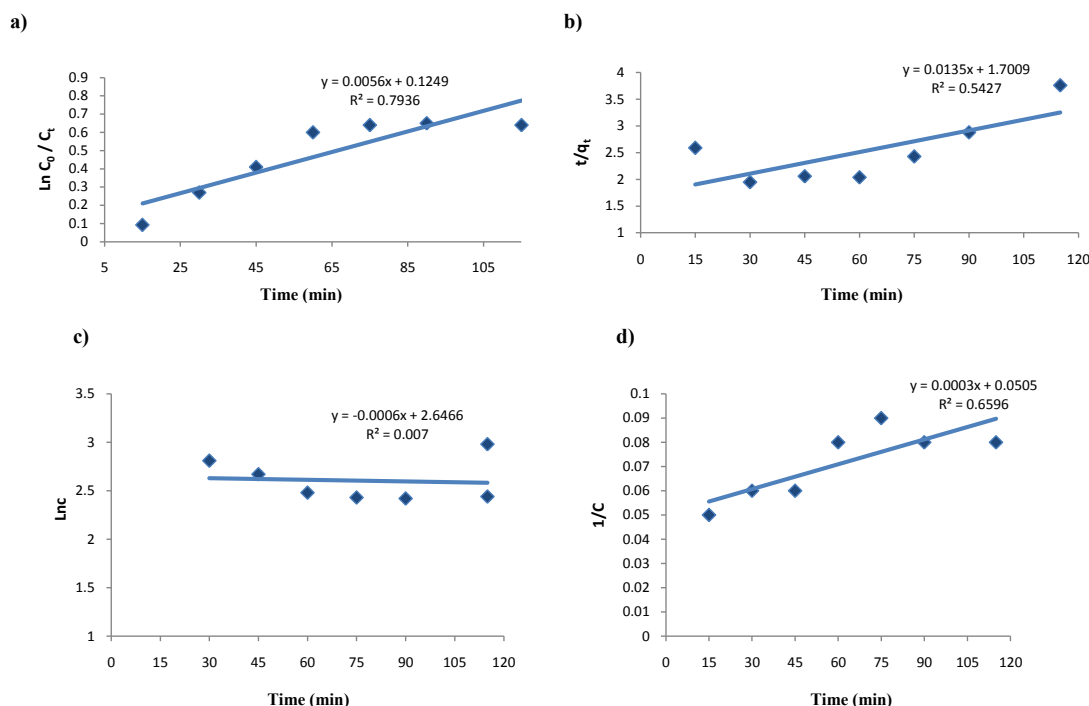


Fig. 7. Kinetic a) pseudo-first-order, b) pseudo-second-order, c) first-order and d) second-order for RBB degradation using SnO.

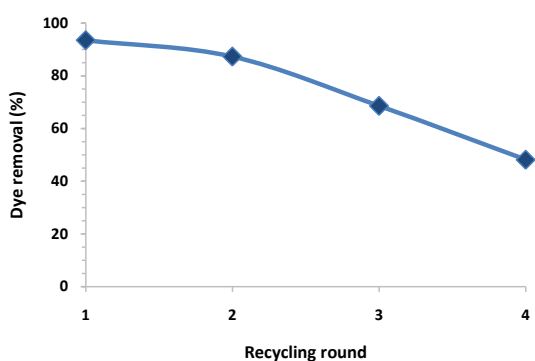


Fig. 8. Recycling round of SnO on RBB photodegradation.

results show that the photocatalyst can be reused for RBB photodegradation.

## CONCLUSIONS

Tin (II) oxide nanosheet has been prepared using a simple reflux in the presence of the ionic liquid. This method produces SnO in good yield with no requirement of high temperature/pressure and calcination. This study demonstrates the 1-pentyl-3-methylimidazolium bromide may be a suitable template for the formation of SnO with nanosheet morphology. Different molar ratio of ionic liquid and sodium hydroxide in the presence of  $\text{SnCl}_2 \cdot 2\text{H}_2\text{O}$  were investigated for preparation of

SnO with different size and morphology. The results show that SnO with high purity and uniform size distribution was obtained using 1:4:4 molar ratios of  $\text{SnCl}_2/\text{NaOH}/\text{IL}$  by simple reflux method. X-ray diffraction (XRD) analysis confirmed the crystalline nature of SnO with orientation in (001), (101), (110), (002), (200), (112) and (103) planes at 18.39, 29.86, 33.30, 37.27, 47.91, 50.83 and 57.40° values. Microflowers with nanosheet subunits (thickness of sheets ~60 nm) were elucidated by scanning electron microscope (SEM). The products may be good candidates for photocatalytic applications in dye removal.

## CONFLICT OF INTEREST

The authors declare that there is no conflict of interests regarding the publication of this manuscript.

## REFERENCES

1. L.Y. Liang, Z.M. Liu, H.T. Cao, Y.Y. Shi, X.L. Sun, Z. Yu, A.H. Chen, H.Z. Zhang and Y.Q. Fang, *ACS Appl. Mater. Interfaces*, 2, 1565 (2010).
2. S.H. Park, Y.C. Son, W.S. Willis, S.L. Suib and K.E. Creasy, *Chem. Mater.*, 10, 2389 (1998).
3. S. Seal and S. Shukla, *JOM.*, 54, 35 (2002).
4. A. Shanmugasundaram, P. Basak, L. Satyanarayana and S.V. Manorama, *Sens. Actuators B.*, 185, 265 (2013).
5. K. Nejati, *Cryst. Res. Technol.*, 47(5), 567 (2012).

6. M. Aziz, S. Saber Abbas, W. Rosemaria and W. Baharom, *Mater. Lett.*, 91, 31 (2013).
7. S. Majumdar, S. Chakraborty, P.S. Devi and A. Sen, *Mater. Lett.*, 62 (8-9), 1249 (2008).
8. D. Han, Y. Wang, C. Sun, B. Liang and W. Zhang, *Ceram. Int.*, 45(3), 4089 (2019).
9. S-Z. Kang, Y. Yang and J. Mu, *Colloids and Surf. A: Physicochemical and Engineering Aspects*, 298(3), 280 (2007).
10. S.P. Choudhury, S.D. Gunjal, N. Kumari, K.D. Diwate, K.C. Mohite and A. Bhattacharjee, *Mater. Today Proceeding* 3(6), 1609 (2016).
11. M.A. El Khakani, R. Dolbec, A.M. Serventi, M.C. Horrillo, M. Trudeau, R.G. Saint-Jacques, D.G. Rickerby and I. Sayago, *Sensors and Actuators B Chemical*, 77(1), 383 (2001).
12. D. Leng, L. Wu, H. Jiang, Y. Zhao, J. Zhang, W. Li and L. Feng, *Int. J. Photoenergy* doi: 10.1155/2012/235971 (2012).
13. Z.R. Dai, Z.W. Pan and Z.L. Wang, *J. Am. Chem. Soc.*, 124, 8673 (2002).
14. M.O. Orlandi, E.R. Leite, R. Aguiar, J. Bettini and E. Longo, *J. Phys. Chem. B*, 110, 6621 (2006).
15. H. Uchiyama, H. Ohgi and H. Imai, *Cryst. Growth. Des.*, 6, 2186 (2006).
16. M.Z. Iqbal, F.P. Wang, T. Feng, H.L. Zhao, M.Y. Rafique, R.U. Din, M.H. Farooq, Q.U. Javed and D.F. Khan, *Mater. Res. Bull.*, 47, 3902 (2012).
17. B. Kumar, D.H. Lee, S.H. Kim, B. Yang, S. Maeng and S.W. Kim, *J. Phys. Chem. C*, 114, 11050 (2010).
18. P. Wasserscheid and T. Welton, Wiley, Weinheim (2003).
19. J. Dupont, R.F. de Souza and P.A.Z. Suarez, *Chem. Rev.*, 102, 3667 (2002).
20. Q. Li, V. Kumar, Y. Li, H. Zhang, T.J. Marks and R.P.H. Chang, *Chem. Mater.*, 17, 1001 (2005).
21. S. Sheshmani and M. Nayebi, *Polym. Composites*, 210 (2019).
22. S.K. Kansal, M. Singh and D. Sud, *J. Hazard. Mater.*, 141(3), 581 (2007).
23. S.M. Hassan and M.A. Mannaa, *Int. J. Nano and Mater. Sci.*, 5(1), 9 (2016).
24. N. Assi, P. Aberoomand Azar, M. Saber Tehrani, S.W. Husain, M. Darwish and S. Pourmand, *Int. J. Nano Dimens.*, 8(3), 241 (2017).
25. A. Radhakrishnan, P. Rejani and B. Beena, *Int. J. Nano Dimens.*, 9(2), 145 (2018).
26. S. Majumdar, *Ceram. Int.*, 41, 14350 (2015).
27. B. Munirathinam, H. Pydimukkala, N. Ramaswamy and L. Neelakantan, *Appl. Surf. Sci.*, 355, 1245 (2015).
28. M. Sabbaghan, A.S. Shahvelayati and S. Banihashem, *Ceram. Int.*, 42, 3820 (2016).
29. M. Sabbaghan, A.S. Shahvelayati and K. Madankar K., *Spectrochimica Acta Part A: Molecular and Biomolecular Spectrosc.*, 135, 662 (2015).
30. M. Sabbaghan, A.S. Shahvelayati and S.E. Bashtani, *Solid State Sci.*, 14, 1191 (2012).
31. M. Obaidullah, M.J. Miah, M.N. Kayes, N. Suzuki and M.M. Hossain, *J. Adv. Chem. Sci.*, 3(1), 445 (2017).
32. M.J. Miah, M.T. Aziz, M.N. Kayes, M. Obaidullah and M.M. Hossain, *British J. Environ. Sci.*, 5(2), 51 (2017).
33. S.K. Kansal, N. Kaur and S. Singh, *Nanoscale Res. Lett.*, 4(7), 709 (2009).
34. S.R. Khan, M.U. Khalid, S. Jamil, S. Li, A. Mujahid and M.R.S. Ashraf Janjua, *J. Water and Health*, 16, 773 (2018).
35. H. Saroyan, D. Ntagiou, K. Rekos and E. Deliyanni, *Appl. Sci.*, 9(10), 2167 (2019).
36. M.P.C. Rao, K. Kulandaivelu, V.K. Ponnusamy, J.J. Wu, A. Sambandam, *Environ. Sci. Pollut. Res.* Doi:10.1007/s11356-019-05434-1 (2019).
37. Y.S. Vygodskii, E.I. Lozinskaya and A.S. Shaplov, *Macromol. Rapid. Commun.*, 676 (2002).
38. A. A. Christy, O.M. Kvalheim and R.A. Velapoldi, *Vib. Spectrosc.*, 9, 19 (1995).
39. K.M. Reddy, S.V. Manorama and A.R. Reddy, (2003), *Mater. Chem. Phys.*, 78, 239 (2003).
40. J. Tauc, R. Grigorov and A. Vancu, *Phys. Status. Solidi*, 15, 627 (1966).